Journal of Pathology
J Pathol 2015; **236:** 136–141
Published online 26 March 2015 in Wiley Online Library (wileyonlinelibrary.com) DOI: 10.1002/path.4522

BRIEF DEFINITIVE REPORT

Recurrent genomic rearrangements in primary testicular lymphoma

David DW Twa,[1,2#] Anja Mottok,[1,2#] Fong Chun Chan,[1,3#] Susana Ben-Neriah,[1] Bruce W Woolcock,[1] King L Tan,[1] Andrew J Mungall,[1,4] Helen McDonald,[4] Yongjun Zhao,[4] Raymond S Lim,[1] Brad H Nelson,[5,6] Katy Milne,[5] Sohrab P Shah,[1,3] Ryan D Morin,[1,7] Marco A Marra,[1,4] David W Scott,[1] Randy D Gascoyne[1,2] and Christian Steidl[1,2*]

[1] *Department of Lymphoid Cancer Research, BC Cancer Agency, Vancouver, BC, Canada*
[2] *Department of Pathology and Laboratory Medicine, University of British Columbia, Vancouver, BC, Canada*
[3] *Bioinformatics Training Programme, University of British Columbia, Vancouver, BC, Canada*
[4] *Canada's Michael Smith Genome Sciences Centre, BC Cancer Agency, Vancouver, BC, Canada*
[5] *Deeley Research Centre, BC Cancer Agency, Victoria, BC, Canada*
[6] *Department of Medical Genetics, University of British Columbia, Vancouver, BC, Canada*
[7] *Department of Molecular Biology and Biochemistry, Simon Fraser University, Vancouver, BC, Canada*

**Correspondence to: C Steidl, Department of Lymphoid Cancer Research, BC Cancer Research Centre, 675 West 10th Avenue, Vancouver, BC V5Z 1 L3, Canada. E-mail: csteidl@bccancer.bc.ca*

[#]These authors contributed equally to this study.

Abstract

Primary testicular diffuse large B cell lymphoma (PTL) is an aggressive malignancy that occurs in the immune-privileged anatomical site of the testis. We have previously shown that structural genomic rearrangements involving the MHC class II transactivator *CIITA* and programmed death ligands (PDLs) 1 and 2 are frequent across multiple B cell lymphoma entities. Specifically in PTL, we found rearrangements in the PDL locus by fluorescence *in situ* hybridization (FISH). However, breakpoint anatomy and rearrangement partners were undetermined, while *CIITA* rearrangements had not been reported previously in PTL. Here, we performed bacterial artificial chromosome capture sequencing on three archival, formalin-fixed, paraffin-embedded tissue biopsies, interrogating 20 known rearrangement hotspots in B cell lymphomas. We report novel *CIITA*, *FOXP1* and PDL rearrangements involving *IGHG4*, *FLJ45248*, *RFX3*, *SMARCA2* and *SNX29*. Moreover, we present immunohistochemistry data supporting the association between PDL rearrangements and increased protein expression. Finally, using FISH, we show that *CIITA* (8/82; 10%) and *FOXP1* (5/74; 7%) rearrangements are recurrent in PTL. In summary, we describe rearrangement frequencies and novel rearrangement partners of the *CIITA*, *FOXP1* and PDL loci at base-pair resolution in a rare, aggressive lymphoma. Our data suggest immune-checkpoint inhibitor therapy as a promising intervention for PTL patients harbouring PDL rearrangements.

Keywords: capture sequencing; fluorescence *in situ* hybridization (FISH); primary testicular lymphoma (PTL); genomic rearrangements; programmed death ligands; *CD274*; *CIITA*; *FOXP1*; *PDCD1LG2*

Received 15 December 2014; Revised 5 February 2015; Accepted 18 February 2015

No conflicts of interest were declared.

Introduction

Primary testicular diffuse large B cell lymphoma (PTL) accounts for 1–2% of all non-Hodgkin's lymphomas [1]. Using gene expression and/or immunohistochemistry-based assays, most of these malignancies are assigned to the activated B cell (ABC)-like cell-of-origin subtype [1–3]. Although incompletely understood, studies have shown that genomic mutations in PTL are diverse, consisting of *B2M* loss-of-function mutations, gain-of-function mutations in *MYD88* and *CD79B*, rearrangements of *BCL2*, *BCL6*, *BCL10*, *CCND1*, *MALT1* and *MYC* and broad deletions of the HLA loci [2,4–7]. PTL also likely exploits limited immune surveillance endogenous to testicular tissue [1]. As a result of these features and the high prevalence of non-germinal centre/ABC subtypes, PTL patients continue to experience a poor prognosis with frequent central nervous system relapse in spite of immunotherapeutic advances [8].

Previously, we have shown via fluorescence *in situ* hybridization (FISH) that the programmed death ligand (PDL) locus is structurally altered across several B cell lymphomas and results in aberrant *CD274* (PD-L1) and *PDCD1LG2* (PD-L2) expression [9]. In PTL, we found an aberration frequency (including copy number

variations and rearrangements) of 49%, although rearrangement anatomy and breakpoint partners were undetermined [9]. Here, using bacterial artificial chromosome (BAC) capture to enrich for predefined genomic loci of interest prior to high-throughput sequencing, we report new structural categories of PDL rearrangement and novel rearrangement partners. Furthermore, we show that these rearrangements lead to increased PDL protein expression in clinical specimens. Finally, we show for the first time that *CIITA* and *FOXP1* rearrangements exist and occur recurrently in PTL.

Methods

To explore novel structural genomic rearrangement partners and breakpoints in PTL, three pretreatment biopsies, one of which was previously shown to be 9p24.1 rearranged by FISH, were selected for targeted BAC capture high-throughput sequencing [9]. One extranodal diffuse large B cell lymphoma (DLBCL), known to harbour a *TBL1XR1–TP63* inversion and *BCL2* rearrangement, was sequenced as a positive control [10]. DNA was extracted from these archival, formalin-fixed, paraffin-embedded (FFPE) tissue samples, using the Qiagen QIAamp DNA FFPE Tissue Kit, according to the manufacturer's protocol, and 2 µg aliquots were used for library construction; 72 BACs tiling 7.45 Mb across 20 genomic regions on 10 different chromosomes known to be recurrently affected by rearrangements in B cell lymphomas were selected to enrich the libraries (Figure 1; see also supplementary material, Table S1) [11]. Paired-end sequencing (75 bp) was performed on an Illumina Hi-Seq2000 and analysed using the nFuse and deStruct algorithms to generate and cross-corroborate rearrangement predictions, as has been published previously [9,12]. These predictions were subsequently filtered on the basis of the validation probability metric (>0.75), a score of uniqueness among libraries, quality and number of spanning and split read support, and alignment relative to the capture space (see supplementary material, Table S2). Subsequently, these events were assessed by BLAT (Blast-like alignment tool) and a select number were validated by Sanger sequencing (see supplementary material, Table S3).

Immunohistochemistry (IHC) for cell-of-origin determination and CD274 and PDCD1LG2 expression was performed on the three capture-sequenced specimens (Table S4–S6). *CIITA* and *FOXP1* FISH break-apart analyses were performed on 88 specimens for which the PDL FISH rearrangement status has been previously reported [9]. We analysed these cases using the same FISH methods and similar criteria and thresholds as we have employed previously to detect the prevalence of *CIITA* and PDL rearrangements [9,13]. This study abided by the Declaration of Helsinki and was approved by the BC Cancer Agency Research Ethics Board (Approval No. H11-00684); please see the online supplementary material for additional details.

Results and discussion

BAC capture sequencing of FFPE tissues yielded a mean coverage depth of 82x across the capture space in the four enriched libraries; 16.7% of reads were non-PCR duplicates that aligned to hg19/GRCh37 (see supplementary material, Figures S1, S2). Following stringent filtering, a list of 16 genomic rearrangements in the four libraries was generated (see supplementary material, Table S2). In the extranodal DLBCL positive control, we observed a *TBL1XR1–TP63* inversion and a *BCL2–IGHV3-9* translocation, validating previously published FISH data [10]. Rearrangement partners, genomic breakpoints and putative translation of the other 14 rearrangement events are presented in Table 1 and Figure 1.

In case A, we identified a translocation between the 5′ intergenic space of *IGHG4* (14q32.33) and the 3′ intergenic space of *PDCD1LG2* (Figure 2). This telomeric repositioning of the PDL locus to chromosome 14 places *PDCD1LG2* under the control of *IGH*-enhancing elements, in line with the classical mechanism of oncogene expression in other B cell lymphomas. This event is also similar to a translocation we have observed in the classical Hodgkin's lymphoma (CHL) cell line L-1236 [9]. Additionally, two interstitial deletions were observed. One deletion involved the 3′ untranslated region (UTR) of *CD274* and the other encompassed exons 5–7 of *PDCD1LG2*. The partial or complete loss of exon 7 for both *CD274* and *PDCD1LG2* has now been observed across three different lymphomas, including CHL, primary mediastinal large B cell lymphoma and PTL [9,14].

Two PDL rearrangements were observed in case B that was negative for PDL rearrangement by FISH. The first event consisted of a deletion joining the 3′ UTRs of *RFX3* (9p24.2; negative strand) and *CD274*. While the literature suggests that a loss of *RFX3* may be advantageous to the tumour, the functional consequences of this rearrangement on the PDL locus remain unclear [15]. As this rearrangement deletes the *CD274* coding sequence, this may suggest an allelic exclusion-like event whereby the malignant cells preferentially select for expression of PDCD1LG2. The second observed PDL event was an inversion between the *SMARCA2* (9p24.3) 5′ intergenic space and *CD274*, simultaneously removing a portion of the 3′ UTR of *CD274*.

IHC revealed that rearrangements of the PDL locus, as present in cases A and B, are associated with increased protein expression, compared with case C, which lacks PDL rearrangement (Figure 3). These observations suggest that, in addition to previously described copy number variations of translocations involving the 9p24.1 locus, inversions and deletions are also capable of increasing PDL protein expression. Furthermore, rearrangements that are undetectable by FISH, due to rearrangement anatomy, and design and resolution of FISH probes, are likewise capable of inducing aberrant surface PDL expression.

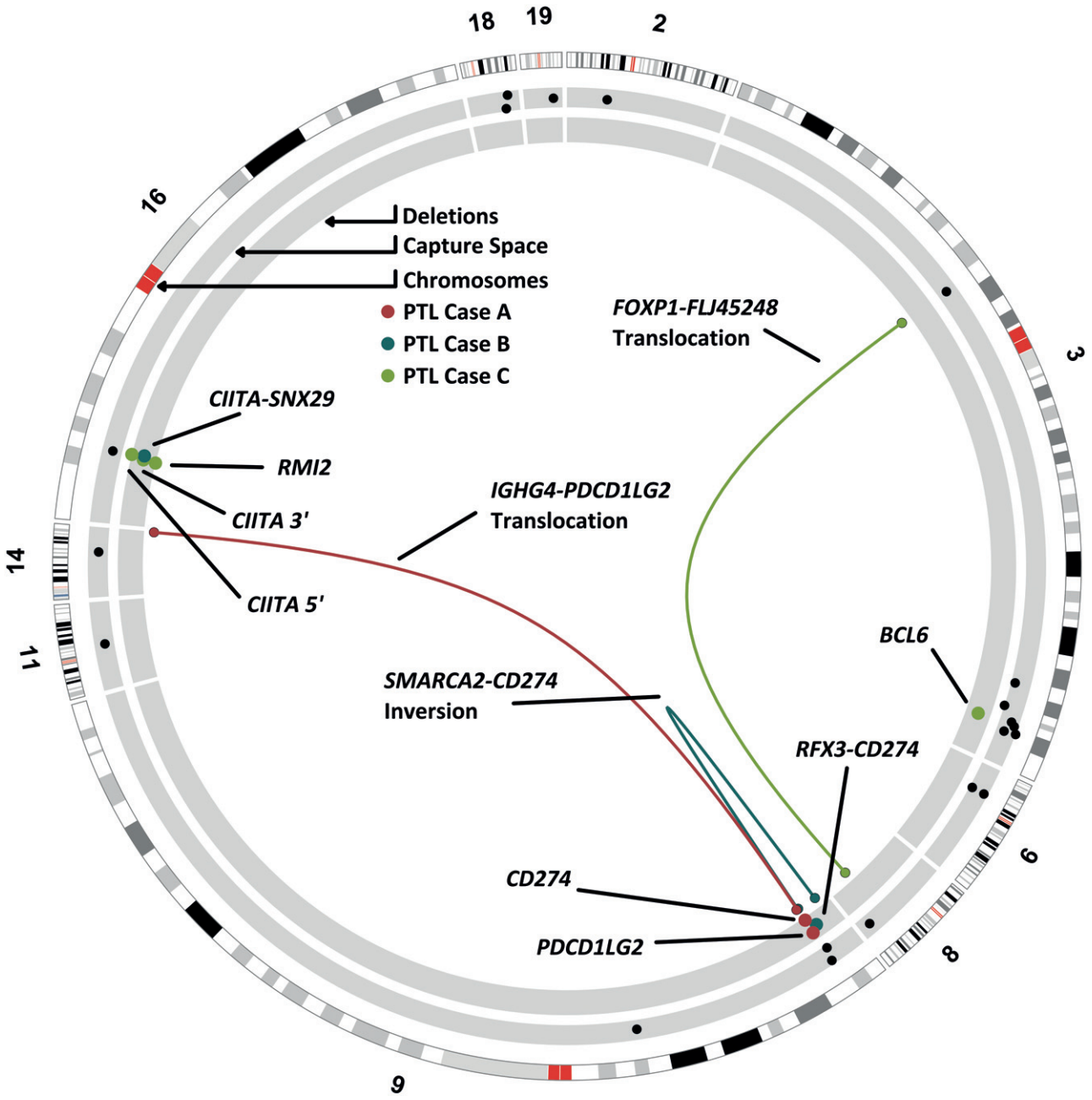

Figure 1. Circos plot depicting the 20 regions of BAC capture space spanning 7.45 Mb and the 11 observed structural genomic events in three libraries obtained from PTL archival FFPE tissue: outer-most concentric track, chromosomes; middle track, capture space (for additional details see supplementary material, Table S1); inner-most track, deletion events; adjoining lines depict rearrangement partners; events are colour-coded to reflect those which overlap between cases. Only chromosomes relevant to the capture space have been included and chromosomes 3, 9 and 16 have been magnified to improve resolution between adjacent events; regions of the chromosomes highlighted in red are the centromeres.

In addition to PDL aberrations, we identified rearrangements of the *CIITA* locus. In case B, we observed an interstitial deletion juxtaposing intron 15 of *CIITA* with intron 14 of *SNX29* (16p13.13). This deletion results in a partial transcriptional loss of the C-terminal leucine-rich repeat domain and putatively produces an out-of-frame fusion leading to a premature stop; this may result in a dominant-negative CIITA protein [13]. In case C, we observed bi-allelic deletions of *CIITA*, which likely cripple normal function of the protein. The 30 kb deletion on one allele includes both promoter regions (III and IV) crucial for transcription in a B cell context, while the deletion on the other allele likely results in an in-frame splice variant of exon 1 to exon 10 that lacks the functionally relevant acidic domain. Inexplicably, these events were not sizeable enough to explain the unbalanced signal pattern observed using FISH, suggesting that a more complex rearrangement may be present. Extending our study of *CIITA* rearrangements in PTL, we performed FISH on an additional 88 specimens, using a previously reported *CIITA* break-apart assay (see supplementary material, Figure S3) [13]. In

Table 1. List of structural genomic rearrangements, as derived from bacterial artificial chromosome capture sequencing of three primary testicular lymphoma libraries obtained from archival, formalin-fixed, paraffin-embedded tissue.

Library	Involved genes	Structural rearrangement type	Genomic location	Exact genomic breakpoints	Putative translational significance	Sanger sequencing validated
A	*CD274*	Interstitial deletion	Exon 7–3′ intergenic	chr9:5468110–chr9:5489373	IE; transcript stability	Y
	PDCD1LG2	Interstitial deletion	Intron 4–Exon 7	chr9:5554986–chr9:5570162	IE; protein solubility	Y
	IGHG4–PDCD1LG2	Translocation	5′ intergenic–3 intergenic	chr14:106094861–chr9:5572111	IE	Y*
B	*CIITA–SNX29*	Interstitial deletion	Intron 15–Intron 14	chr16:11011017–chr16:12330239	DN; reduced MHCII	Y*
	SMARCA2–CD274	Inversion	5′ intergenic–Exon 7	chr9:1948958–chr9:5468076	IE; transcript stability	N
	RFX3–CD274	Interstitial deletion	Exon 16–Exon 7	chr9:3220442–chr9:5468461	IE of PDCD1LG2	Y
C	*CIITA*	Interstitial deletion	5′ intergenic–Intron 3	chr16:10960096–chr16:10990709	DE; reduced MHCII	Y
	CIITA	Interstitial deletion	Intron 1–Intron 9	chr16:10988710–chr16:10997807	DN; reduced MHCII	Y
	FOXP1–FLJ45248	Translocation	Intron 11–3′ intergenic	chr3:71074272–chr8:103828413	IE; proapoptotic repression	N*
	BCL6	Interstitial deletion	5′ intergenic–Intron 1	chr3:187461229–chr3:187463676	IE; cell cycle progression	N
	RMI2	Interstitial deletion	Intron 1–Intron 2	chr16:11389010–chr16:11389154	DE; genomic instability	N

The genomic location column presents the site of the genomic break, while the putative translational significance column lists the predicted effect of the rearrangement based on the literature.
DE, decreased expression; DN, dominant-negative phenotype; IE, increased expression; Y, validated; N, not validated, due to exhaustion of available genomic material.
*Also observed via fluorescence *in situ* hybridization.

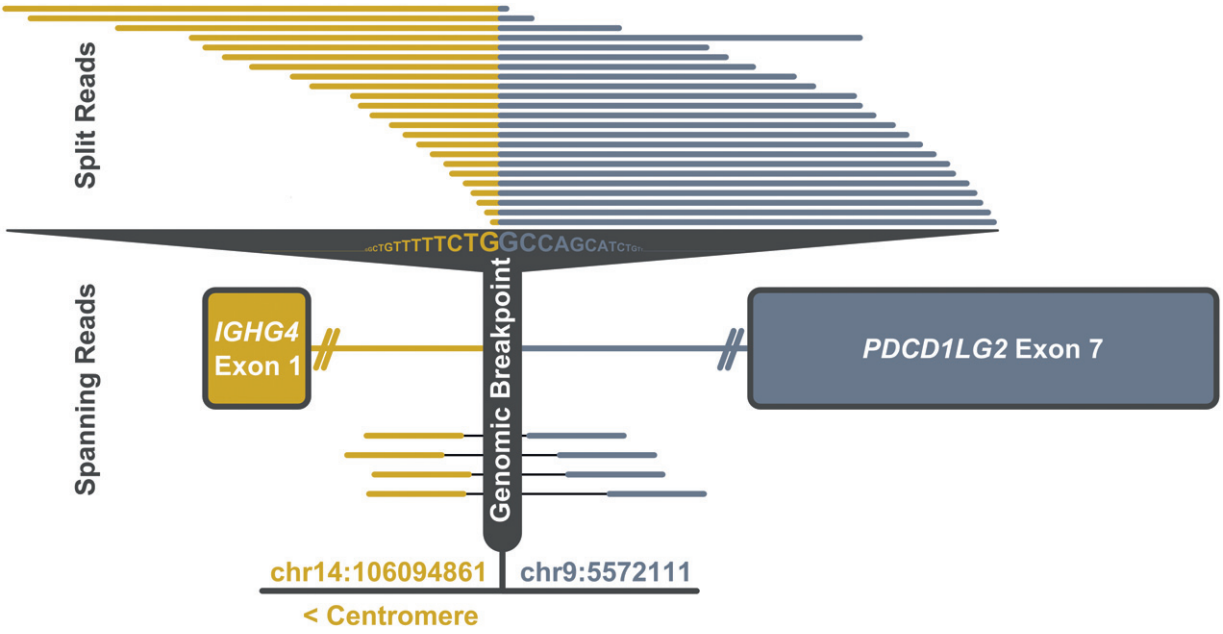

Figure 2. Genomic breakpoint plot depicting the split and spanning read support for the *IGHG4–PDCD1LG2* translocation in case A. Exon lengths, split and spanning reads are mapped relative to one another; however, the intergenic space between the exons is not to scale, due to the distance of the genomic breakpoint from the exons.

total, we observed a break-apart signal pattern in 8/82 (10%) of evaluable cases, suggesting that *CIITA* rearrangements are recurrent and may be responsible for reduced levels of MHC class II expression in a subset of PTLs [7].

In case C, we also observed three other rearrangements: a loss of the *BCL6* exon 1 which likely contributes to deregulation of BCL6 autoregulation, as has been ascribed to exon 1 point mutations of *BCL6*; an exon 2 deletion of *RMI2*, presently of unknown consequence; and a complex *FOXP1* translocation [16]. *FOXP1* has been described as an oncogene that is capable of repressing the apoptotic pathway in B cells and is known to be rearranged in several B cell lymphoma entities [17,18]. Specifically, the translocation between *FOXP1* and *FLJ45248* (8q22.3) substantially attenuates the 5′ coding sequence of *FOXP1* and could be categorized as an N-truncated non-*IGH–FOXP1* rearrangement, as has been described previously [19]. To assess the recurrence of *FOXP1* rearrangements, we performed break-apart FISH on 88 PTLs (see supplementary material, Figures S3, S4) and determined a cumulative rearrangement frequency of 5/74 (7%). This suggests that rearrangement may serve as one potential mechanism for inducing FOXP1 protein expression characteristic of PTL [1,2].

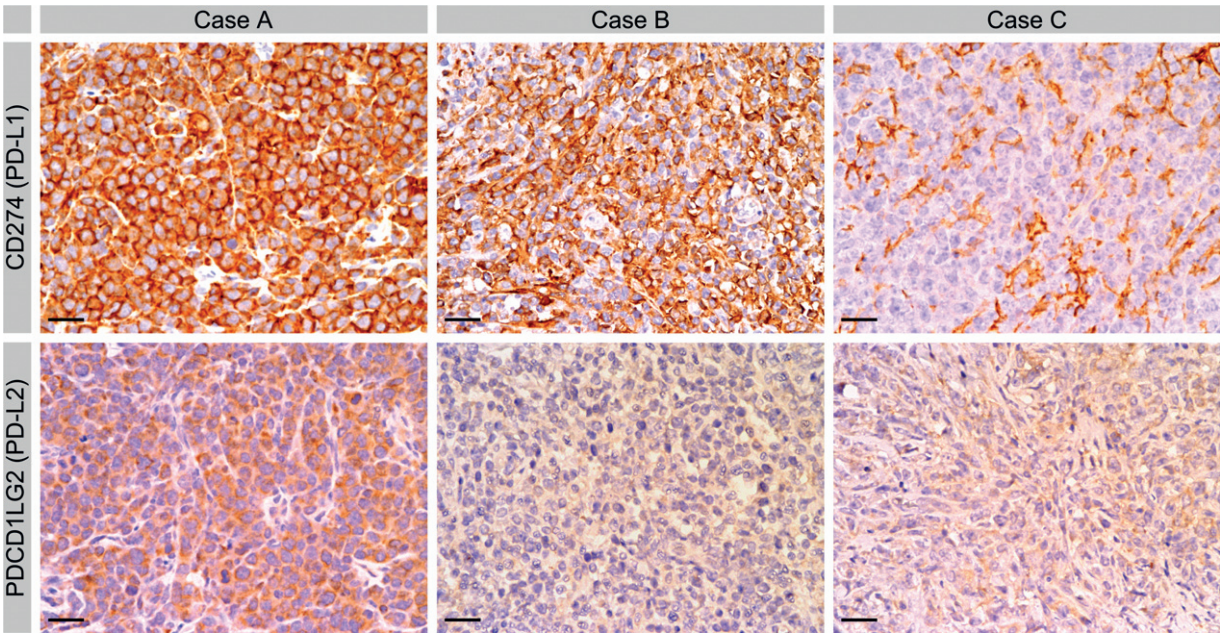

Figure 3. CD274 and PDCD1LG2 immunohistochemistry staining patterns for the three capture-sequenced PTL cases. Intense membranous staining for CD274 and PDCD1LG2 in case A and CD274 in case B can be observed in comparison to case C, which harbours no apparent structural genomic aberration. The over-expression of PDL protein in cases A and B informs on the functional consequences of the deletions, inversion and translocation involving the PDL genes. Representative pictures were taken using a Nikon Eclipse E600 microscope equipped with a Nikon DS-Fi1 camera at room temperature; original magnification = ×400; black bar = 50 μm.

Our findings demonstrate, at base-pair-level resolution, several novel structural genomic rearrangements in PTL. Previously detailed breakpoint biology of these loci was limited to more prevalent B cell lymphoma entities with available fresh-frozen material. Here, we have shown the feasibility of using archival FFPE tissue to identify novel genomic rearrangements through capture-based, high-throughput, sequencing techniques to supplement FISH observations. We have reported two novel rearrangement types (deletions and inversions) and three new partners (*IGHG4*, *RFX3* and *SMARCA2*) of PDLs and have demonstrated that these rearrangements substantially alter protein expression in primary tissue samples. We have also shown that, while PDLs do not appear to rearrange consistently with one genomic partner, deletion of 3′ UTRs in both *CD274* and *PDCD1LG2* across subsets of B cell lymphomas is recurrent. Finally, we have shown that *CIITA* and *FOXP1* rearrangements in PTL are present at frequencies of 10% and 7%, respectively. Taken together, our findings suggest that immune-checkpoint inhibitor therapy targeting PDLs and/or their cognate receptor PDCD1 might be a rational choice for PTL patients, particularly for those individuals harbouring PDL locus alterations and/or high surface expression of PDLs [20].

Acknowledgements

Funds supporting this research were provided by the Canadian Institutes of Health Research (CIHR), the Terry Fox Research Institute (Grant No. 1023, to RDG and CS), the Canadian Cancer Society (Grant No. 702519 to CS), and the BC Cancer Foundation. CS is also a recipient of a Career Investigator Award from the Michael Smith Foundation for Health Research; AM is supported by a Mildred Scheel Cancer Foundation Fellowship; and DDWT is supported by a University of British Columbia Fellowship, a Killam Foundation Doctoral Scholarship and a CIHR Vanier Doctoral Scholarship. The authors would also like to thank the Biospecimen, Library Construction and Sequencing cores of Canada's Michael Smith Genome Sciences Centre for their technical assistance and Gordon J Freeman of the Dana-Farber Cancer Center for generously providing the PDCD1LG2 antibody.

Author contributions

DDWT, AM and FCC each contributed equally in designing and performing the research, interpreting the data and writing and editing the manuscript; SBN and KLT specifically produced and analysed FISH data; BWW produced and analysed sequencing data; AJM, HD and YZ generated BAC capture and sequencing data, which was also analysed by RSL; BHN and KM generated and analysed IHC data; SPS, RDM, MAM and DWS provided experimental and editorial input; RDG and CS designed the research, analysed data and wrote the manuscript, and CS also approved the paper.

References

1. Cheah CY, Wirth A, Seymour JF. Primary testicular lymphoma. *Blood* 2014; **123:** 486–493.

2. Bernasconi B, Uccella S, Martin V, *et al.* Gene translocations in testicular lymphomas. *Leuk Lymphoma* 2014; **55:** 1410–1412.
3. Booman M, Szuhai K, Rosenwald A, *et al.* Genomic alterations and gene expression in primary diffuse large B cell lymphomas of immune-privileged sites: the importance of apoptosis and immunomodulatory pathways. *J Pathol* 2008; **216:** 209–217.
4. Jordanova ES, Riemersma SA, Philippo K, *et al.* β2-microglobulin aberrations in diffuse large B-cell lymphoma of the testis and the central nervous system. *Int J Cancer* 2003; **103:** 393–398.
5. Kraan W, van Keimpema M, Horlings HM, *et al.* High prevalence of oncogenic *MYD88* and *CD79B* mutations in primary testicular diffuse large B-cell lymphoma. *Leukemia* 2014; **28:** 719–720.
6. Kuper-Hommel MJ, Schreuder MI, Gemmink AH, *et al.* T(14;18)(q32;q21) involving *MALT1* and *IGH* genes occurs in extranodal diffuse large B-cell lymphomas of the breast and testis. *Mod Pathol* 2013; **26:** 421–427.
7. Riemersma SA, Oudejans JJ, Vonk MJ, *et al.* High numbers of tumour-infiltrating activated cytotoxic T lymphocytes, and frequent loss of HLA class I and II expression, are features of aggressive B cell lymphomas of the brain and testis. *J Pathol* 2005; **206:** 328–336.
8. Villa D, Connors JM, Shenkier TN, *et al.* Incidence and risk factors for central nervous system relapse in patients with diffuse large B-cell lymphoma: the impact of the addition of rituximab to CHOP chemotherapy. *Ann Oncol* 2010; **21:** 1046–1052.
9. Twa DD, Chan FC, Ben-Neriah S, *et al.* Genomic rearrangements involving programmed death ligands are recurrent in primary mediastinal large B-cell lymphoma. *Blood* 2014; **123:** 2062–2065.
10. Scott DW, Mungall KL, Ben-Neriah S, *et al. TBL1XR1/TP63*: a novel recurrent gene fusion in B-cell non-Hodgkin lymphoma. *Blood* 2012; **119:** 4949–4952.
11. Morin RD, Mendez-Lago M, Mungall AJ, *et al.* Frequent mutation of histone-modifying genes in non-Hodgkin lymphoma. *Nature* 2011; **476:** 298–303.
12. McPherson A, Wu C, Wyatt AW, *et al.* nFuse: discovery of complex genomic rearrangements in cancer using high-throughput sequencing. *Genome Res* 2012; **22:** 2250–2261.
13. Steidl C, Shah SP, Woolcock BW, *et al.* MHC class II transactivator CIITA is a recurrent gene fusion partner in lymphoid cancers. *Nature* 2011; **471:** 377–381.
14. Gunawardana J, Chan FC, Telenius A, *et al.* Recurrent somatic mutations of *PTPN1* in primary mediastinal B cell lymphoma and Hodgkin lymphoma. *Nat Genet* 2014; **46:** 329–335.
15. Jia D, Dong R, Jing Y, *et al.* Exome sequencing of hepatoblastoma reveals novel mutations and cancer genes in the Wnt pathway and ubiquitin ligase complex. *Hepatology* 2014; **60:** 1686–1696.
16. Pasqualucci L, Migliazza A, Basso K, *et al.* Mutations of the BCL6 proto-oncogene disrupt its negative autoregulation in diffuse large B-cell lymphoma. *Blood* 2003; **101:** 2914–2923.
17. van Keimpema M, Gruneberg LJ, Mokry M, *et al.* FOXP1 directly represses transcription of proapoptotic genes and cooperates with NF-κB to promote survival of human B cells. *Blood* 2014; **124:** 3431–3440.
18. Haralambieva E, Adam P, Ventura R, *et al.* Genetic rearrangement of FOXP1 is predominantly detected in a subset of diffuse large B-cell lymphomas with extranodal presentation. *Leukemia* 2006; **20:** 1300–1303.
19. Rouhigharabaei L, Finalet Ferreiro J, Tousseyn T, *et al.* Non-IG aberrations of FOXP1 in B-cell malignancies lead to an aberrant expression of *N*-truncated isoforms of FOXP1. *PLoS One* 2014; **9:** e85851.
20. Ansell SM, Lesokhin AM, Borrello I, *et al.* PD-1 Blockade with nivolumab in relapsed or refractory Hodgkin's lymphoma. *N Engl J Med* 2014; **372**: 311–319.

SUPPLEMENTARY MATERIAL ON THE INTERNET

The following supplementary material may be found in the online version of this article:

Supplementary materials and methods

Figure S1. Total number of reads and mean coverage per BAC capture library

Figure S2. Mean coverage per capture space across all four libraries

Figure S3. Representative FISH break-apart signal patterns observed in PTL samples

Figure S4. BAC probe design for the *FOXP1* (chr3p13) FISH break-apart assay

Table S1. The bacterial artificial chromosomal capture space encompassing 72 probes for capture sequencing

Table S2. The nFuse output of filtered rearrangement sequences in the three PTL libraries and extranodal diffuse large B-cell lymphoma positive control

Table S3. M13 tagged primers used for Sanger sequencing validation of select rearrangement predictions derived from capture sequencing

Table S4. Cell-of-origin (Hans algorithm) and additional known genetic aberrations present in the three PTLs and extranodal diffuse large B cell lymphoma positive control

Table S5. Extension cohort of PTL cases used for FISH break-apart assays

Table S6. Comprehensive list of antibodies used to determine cell of origin and inform on the expression of PDLs in the three capture-sequenced PTLs